JOURNAL OF GEOPHYSICAL RESEARCH, VOL. 107, NO. D23, 4715, doi:10.1029/2002JD002272, 2002

Stability of tropospheric hydroxyl chemistry

J. Lelieveld,[1] W. Peters,[2] F. J. Dentener,[3] and M. C. Krol[2]

Received 6 March 2002; revised 1 August 2002; accepted 22 August 2002; published 12 December 2002.

[1] Tropospheric hydroxyl (OH) is the cleaning agent of the atmosphere, because most oxidation processes are initiated by OH. If the OH chemical system were unstable, runaway growth of oxidants (autocatalytic conditions) or of reduced gases (catastrophic conditions) might occur, especially because the atmospheric composition is changing rapidly. We present simulations with a global chemistry-transport model, indicating that during the past century, global mean OH has nevertheless remained nearly constant. This constancy is remarkable, because CH_4 and CO, the main OH sinks, have increased strongly. We studied the system's sensitivity to perturbations using the OH recycling probability, calculated from primary OH formation and OH recycling. We conclude that the constancy of global mean OH does not imply that regional OH has not changed or that the system is insensitive to perturbations. Over the tropical oceans, where OH concentrations are highest, the system stability is relatively low. During the past century, the OH concentration decreased substantially in the marine troposphere, however, on a global scale, it has been compensated by an increase over the continents associated with strong pollution emissions of nitrogen oxides. Our results suggest that the changing atmospheric composition due to industrialization has been accompanied with a 60% increase in the tropospheric oxidation power (i.e., gross OH production). *INDEX TERMS:* 0322 Atmospheric Composition and Structure: Constituent sources and sinks; 0365 Atmospheric Composition and Structure: Troposphere—composition and chemistry; 0368 Atmospheric Composition and Structure: Troposphere—constituent transport and chemistry

Citation: Lelieveld, J., W. Peters, F. J. Dentener, and M. C. Krol, Stability of tropospheric hydroxyl chemistry, *J. Geophys. Res.*, *107*(D23), 4715, doi:10.1029/2002JD002272, 2002.

1. Introduction

[2] Atmospheric oxidation processes largely proceed along reaction chains that are initiated by hydroxyl radicals (OH) [*Levy*, 1971]. Although other oxidants can also initiate such reactions, OH is by far dominant so that we focus on this molecule. The primary formation of OH is mediated by ozone (O_3), which, in the stratosphere, is produced from O_2 photodissociation. A small fraction of stratospheric O_3 is transported to the troposphere, which constitutes a baseline OH source. Additionally and most importantly, OH is formed from O_3 that is produced by in situ photochemistry within the troposphere. The reactions are initiated by ultraviolet (UV) sunlight. Figure 1 shows that primary OH formation is controlled by ozone, UV radiation and water vapor in reactions R1,4. UV radiation fluxes, in turn, are strongly dependent on the solar zenith angle and the overhead O_3 column. Therefore OH levels are highest in the tropics where the stratospheric ozone layer is thinnest and the absolute humidity is highest. For a historical overview of the global scale processes involved we refer to *Logan et al.* [1981], *Perner et al.* [1987], *Spivakovsky et al.* [1990, 2000], *Ehhalt et al.* [1991] and *Thompson* [1992]. The tropospheric lifetime of OH is very short, a few seconds, because it rapidly reacts with carbon monoxide (CO) and hydrocarbons, in the background troposphere notably methane (CH_4) [*McConnell et al.*, 1971; *Crutzen*, 1973; *Chameides and Walker*, 1973]. Although CH_4 and CO constitute efficient OH sinks, these reactions do not necessarily deplete OH because part of the radicals can be recycled, e.g., by the action of nitrogen oxides ($NO_x \equiv NO + NO_2$). Figure 1 shows that in the presence of NO, O_3 is produced and OH is reformed through reaction R7 (Cycle 1).

[3] NO_x is removed within a few days, i.e., close to the sources, by the formation of nitric acid (HNO_3), predominantly by reaction with OH, and also through heterogeneous conversion on aerosols and clouds at night. The lifetime of CO, on the other hand, is much longer, about two months, so that it can be transported over thousands of kilometers. The lifetime of CH_4 is about eight years so that it is globally well mixed. In NO_x depleted air far downwind of pollution sources reaction R7 between NO and HO_2 is insignificant and the alternative Cycle 2 prevails (Figure 1). In this case O_3 is destroyed and the HO_x radicals can recombine into hydrogen peroxide (H_2O_2) ($HO_x \equiv OH + HO_2$). This can terminate the radical reaction chain because a large part of the H_2O_2 is removed by dry and wet deposition. While some

[1]Max-Planck-Institute for Chemistry, Mainz, Germany.
[2]Institute for Marine and Atmospheric Research, Utrecht, Netherlands.
[3]Joint Research Centre, Environment Institute, Ispra, Italy.

0148-0227/02/2002JD002272$09.00

Primary OH formation:

R1: $O_3 + h\nu\ (\lambda<330\,nm) \rightarrow O(^1D) + O_2$

R2: $O(^1D) + M \rightarrow O(^3P) + M$ (97%)

R3: $O(^3P) + O_2 + M \rightarrow O_3 + M$

R4: $O(^1D) + H_2O \rightarrow 2OH$ (3%)

OH recycling, O_3 formation (NO_x enriched):

R5: $CO + OH \rightarrow CO_2 + H$

R6: $H + O_2 + M \rightarrow HO_2 + M$

R7: $NO + HO_2 \rightarrow NO_2 + OH$

R8: $NO_2 + h\nu\ (\lambda<420\,nm) \rightarrow NO + O(^3P)$

R3: $O(^3P) + O_2 + M \rightarrow O_3 + M$

Cycle 1: $CO + 2O_2 \rightarrow CO_2 + O_3$

OH recycling, O_3 loss (NO_x depleted):

R5: $CO + OH \rightarrow CO_2 + H$

R6: $H + O_2 + M \rightarrow HO_2 + M$

R9: $O_3 + HO_2 \rightarrow 2O_2 + OH$

Cycle 2: $CO + O_3 \rightarrow CO_2 + O_2$

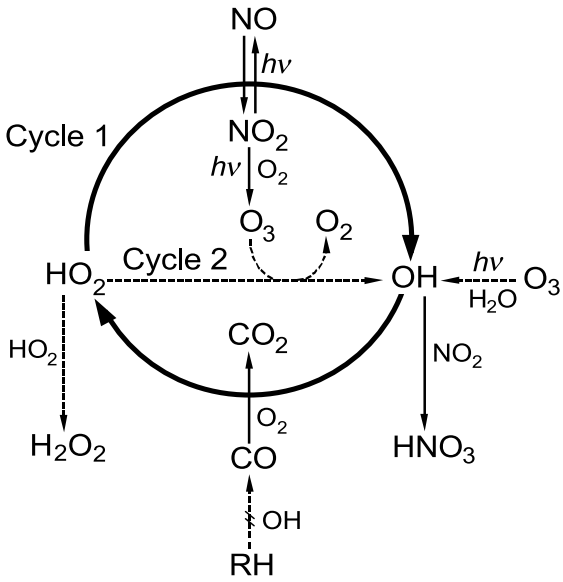

Figure 1. Reaction cycles of OH and HO_2 as determined by reactions with CO and NO_x. RH represents hydrocarbons (on a global scale dominated by CH_4). In reactions R2, 3, 6 collisions with air molecules (M) dissipate excess energy. About 3% of the $O(^1D)$ atoms formed in the troposphere through reaction R1 produces OH. Cycle 1 regenerates OH and produces O_3, while Cycle 2 (dashed) destroys O_3 hence reduces primary OH formation. H_2O_2 and HNO_3 are important sinks of HO_x at NO_x depleted and highly NO_x enriched conditions, respectively.

of the HO_x can be regained from H_2O_2 through photolysis, deposition is a definitive sink for about half the HO_x radicals that form H_2O_2.

[4] The stability of the OH chemical system, as affected by emissions of NO_x, CO and CH_4, has been extensively studied with photochemical box models [*Guthrie*, 1989; *Kleinman*, 1994; *Prather*, 1994; *Stewart*, 1995; *Krol and Poppe*, 1998; *Poppe and Lustfeld*, 1996; *Hess and Madronich*, 1997]. It appears that under NO_x depleted conditions OH recycling is inefficient and HO_2 recombination into H_2O_2 predominates. When concentrations of CO and CH_4 are very high and growing rapidly, such conditions can become catastrophic as both O_3 and HO_x are removed. Conversely, at high NO_x levels when OH recycling is very efficient, the system can become autocatalytic, leading to a runaway of oxidants. Under NO_x enriched conditions OH recycling is quite efficient, however, the reaction between NO_2 and OH gains importance as a sink of HO_x. At very high NO_x mixing ratios (>10 nmol/mol) NO_2 can deplete OH to very low levels. The previously mentioned box model studies have shown that the high NO_x system can become unstable, and that short periods with high (initially autocatalytic) OH formation are followed by long periods of OH suppression. However, in the atmosphere such conditions are likely to be rare and spatially confined since transport and mixing processes lead to rapid dilution.

[5] We have investigated global OH in view of paradoxical reports about historical OH variations. On the one hand, analyses of multiyear methyl chloroform measurements (MCF: 1, 1, 1-trichloroethane), a man-made trace gas that is removed by OH, and of which sources and atmospheric concentrations are well quantified, suggest large OH changes of 5–15% per decade since 1979 [*Krol et al.*, 1998; *Prinn et al.*, 2001]. Re-analysis of the MCF measurements, based on modified MCF emission data, has moderated this conclusion (M. C. Krol et al., Revised OH trends due to persisting methyl chloroform emissions, submitted to *Nature*, 2002, hereinafter referred to as Krol et al., submitted manuscript, 2002) [*Krol and Lelieveld*, 2002]. On the other hand, model simulations constrained by ice core measurements have shown that global OH changes during the past century have probably been small, in spite of CH_4 and CO increases in excess of a factor of two [*Pinto and Khalil*, 1991; *Lelieveld and Van Dorland*, 1995; *Wang and Jacob*, 1998].

[6] Here we present simulations with a global chemistry-transport model to study changes in the concentration and distribution of OH in the troposphere during the past

century. We introduce several concepts to help analyze these changes. The ''oxidation power'' of the troposphere, for example, is defined as the global gross OH formation (the concept is also applied to smaller scales). We avoid using the term ''oxidation efficiency'' because it is often related to a specific compound to be oxidized, and therefore difficult to determine [*Lawrence et al.*, 2001]. We furthermore study the sensitivity of the OH chemical system to perturbations, for which we define the ''OH recycling probability'' (a diagnostic of the instantaneous stability). We differentiate between the instantaneous stability, being the sensitivity to small perturbations in the present or preindustrial atmosphere, and long-term changes. The latter are the result of forcings (e.g., changing emissions) as well as the stability (how does the system respond to a forcing). The first does not account for potentially nonlinear feedbacks on long timescales, while the second takes these into account.

[7] In the next section we describe our model and the emission scenarios. In section 3 we define the OH recycling probability, and first apply it on a single box, representing global mean conditions. Since the system stability depends on the type of perturbation exerted and the ambient conditions, we subsequently analyze all grid boxes of the global model to refine the concept to regional scales. We have performed sensitivity simulations based on NO_x and CH_4 perturbations, which have opposite effects on OH, to explore to what extent the stability analysis can be generalized. In section 4 we discuss OH distribution changes in the past century, and argue that statements about global mean OH changes need to be extended with a regional view. In section 5 we address the role of oxidant transport in maintaining the stability of OH chemistry in the background troposphere. Section 6 presents the conclusions.

2. Model Description

[8] The global chemistry-transport model (Tracer Model version 3; TM3) used has a spatial resolution of 5° longitude, 3.75° latitude and 19 levels up to 10 hPa, and has been tested by comparison with in situ and remote sensing data [*Houweling et al.*, 1998; *Dentener et al.*, 1999; *Lelieveld and Dentener*, 2000; *Peters et al.*, 2001, 2002]. Tracer transport, cloud properties, precipitation, temperature and other physical parameters have been derived from six-hourly mean meteorological fields from the European Centre for Medium-range Weather Forecasts (ECMWF) reanalyses, available for the period 1979–1993 [*Gibson et al.*, 1997]. All model simulations have been performed with a one-year spin-up period.

[9] Stratospheric O_3 above 10 hPa has been prescribed based on Halogen Occultation Experiment (HALOE) satellite measurements. Between 10 and 50 hPa ozone is relaxed toward zonal mean mixing ratios based on measurements by the Total Ozone Mapping Spectrometer (TOMS) and ozone sondes, whereas the 3D ozone variability arises from simulated transports [*Lelieveld and Dentener*, 2000]. Below 50 hPa ozone is calculated without fixed boundary conditions. Methane is prescribed at the surface on the basis of observations, model interpolation and comparison with ice core analyses, being about 0.8 μmol/mol for the preindustrial and about 1.75 μmol/mol for the present-day atmosphere [*Houweling et al.*, 2000].

[10] The chemical scheme accounts for 48 species that describe CH_4-CO-NMHC-NO_x-SO_x chemistry of which 32 are transported (including marked tracers) (NMHC is Nonmethane Hydrocarbons). The model accounts for 24 photodissociation and 67 thermal reactions and heterogeneous processes. The chemistry calculations are performed with a time resolution of 15 min. Photodissociation frequencies are calculated with the routine of *Landgraf and Crutzen* [1998]. The chemistry scheme includes peroxyacetyl nitrate (PAN), which represents the sum of all PAN-like components, as described and evaluated by *Houweling et al.* [1998]. Dry deposition of trace gases and aerosols is simulated according to *Ganzeveld et al.* [1998] and wet deposition is based on the method of *Guelle et al.* [1998]. Dry deposition is an important sink for NO_2, HNO_3, PAN, formaldehyde and acetaldehyde, and wet deposition is important for HNO_3, H_2O_2 and formaldehyde. The chemical mechanism includes the heterogeneous conversion of NO_x to HNO_3 on aerosols according to *Dentener and Crutzen* [1993].

[11] Trace gas emissions are from the Emission Database for Global Atmospheric Research (EDGAR 2.0) [*Olivier et al.*, 1999]. Information about EDGAR is available through http://www.rivm.nl/env/int/coredata/edgar/intro.html. The simulations of preindustrial conditions have been based on the emission data of *Van Aardenne et al.* [2001]. Present-day emissions of CO amount to 585 Tg C yr^{-1} (of which 424 Tg C yr^{-1} are anthropogenic); for the preindustrial conditions this is 303 Tg C yr^{-1} (and 98 Tg C yr^{-1}). Present-day emissions of NMHC are 597 Tg yr^{-1} (190 Tg yr^{-1} anthropogenic); preindustrial NMHC emissions are 430 Tg yr^{-1} (20 Tg yr^{-1} anthropogenic). Present-day NO_x emissions are 45.7 Tg N yr^{-1} (36.3 Tg N yr^{-1} anthropogenic); preindustrial NO_x emissions are 12.9 Tg N yr^{-1} (2.7 Tg N yr^{-1} anthropogenic). These emission estimates have been described in more detail by *Lelieveld and Dentener* [2000]. Biomass burning emissions have been described and evaluated by *Marufu et al.* [2000], and further discussed by *Peters et al.* [2002].

3. OH Recycling Probability

[12] The results of our global model simulations for the present-day troposphere indicate that in total about 92 Tmol yr^{-1} primary OH formation takes place through the photodissociation of O_3 (R1) followed by reaction of $O(^1D)$ + H_2O (R4) (Tmol is 10^{12} mol). Figure 2 presents normalized global mean production and destruction rates of OH and HO_2 in the troposphere (the results from the preindustrial scenario will be discussed in section 4). We calculate that nearly half the OH initially lost in the oxidation of CH_4 and CO is recycled by NO in reaction R7. In the absence of NO regeneration of OH by the reaction with O_3 (R9) is important. Furthermore, many hydrocarbon oxidation pathways lead to OH through the formation and breakdown of oxygenated intermediates such as aldehydes, notably formaldehyde (CH_2O). The OH yield from these intermediates can even overcompensate the OH loss from the initial hydrocarbon attack. The total secondary OH formation, defined as the yield from OH recycling in Cycle 1, 2 and photodissociation of peroxides, is about 96 Tmol yr^{-1}.

[13] Next we define the oxidation power, *G*, being the time rate at which OH is produced (gross OH formation). *G*

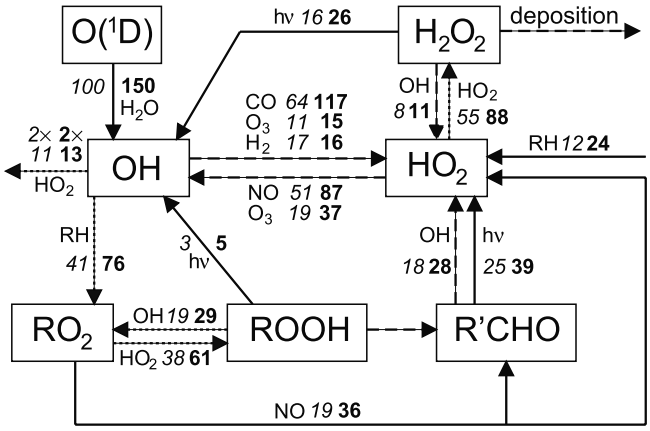

Figure 2. Model calculated global, annual mean HO_x reaction cycle in the troposphere. The numbers represent fractional contributions in percent, scaled to primary OH formation by the reactions R1, 4; 100% represents 62 Tmol yr^{-1} (reaction $O(^1D) + H_2O$ in the preindustrial troposphere). Values for the preindustrial and present-day troposphere are printed in italic (left) and bold (right), respectively. During industrialisation primary OH formation has increased by about 50% and gross OH formation by about 60%. Solid arrows refer to a gain of HO_x, short-dashed to a loss of HO_x, and long-dashed arrows are HO_x neutral. Minor pathways have been accounted for through the major ones.

is the sum of primary (P) and total secondary (S) OH formation. For the whole troposphere G is expressed as a global annual rate (Tmol/year). The OH recycling probability (r) is defined by $r = 1 - P/G$. G is related to P and r by

$$G = P + S = P + rP + r^2P + \ldots = \frac{P}{1-r} \qquad (1)$$

From our model calculations we infer that globally, $G = 188$ Tmol yr^{-1} and $P = 92$ Tmol yr^{-1}, yielding a mean r of about 0.5. By considering the global troposphere as a well-mixed reaction vessel, it would follow that the system could become autocatalytic if r approaches 1. The result that $r \approx 0.5$ implies that tropospheric OH formation is quite efficient but not autocatalytic. The global OH chemical system may thus appear to be stable so that perturbations by CH_4 and CO are expected to cause only small or moderate OH changes, depending on the system forcing. At low r OH concentrations could become very sensitive to CH_4 and CO changes. Under low-r conditions OH production strongly depends on primary production, so that it is most sensitive to changes in O_3 photolysis rates (UV radiation), ozone and water vapor. Under high-r conditions the system is insensitive against perturbations of primary OH formation, however, at $r \rightarrow 1$ runaway oxidant build-up may result from secondary OH formation.

[14] In addition to global mean values of r in a box-model approach, this quantity can also be evaluated for much smaller scales using local OH production and recycling rates. This is viable because OH is entirely determined by local chemical conditions. Figure 3 presents model calculated annual mean OH in the boundary layer, showing that OH can vary up to an order of magnitude over single latitudes, which illustrates the geographical OH dependence and the importance of local conditions. Note that in this article we focus on the middle and low latitudes, limiting ourselves to the model domain in which annual average primary OH formation exceeds 0.55 nmol/mol s^{-1}. This appears to encompass 74% of the Earth's surface. In the discussion we thus exclude conditions that only marginally affect the tropospheric oxidation power. The latter typically applies to high latitudes (higher than about 50–60° latitude), where annual mean OH concentrations are below 10^5 molecules cm^{-3} (Figure 3). Most examples used in this article pertain to the boundary layer because the contrasts between polluted and clean air and the sensitivity to trace gas emissions appear to be largest near the surface.

[15] Figure 4 shows model results for r as a function of NO_x for all boundary layer grid boxes. First we focus on the present-day atmosphere (black dots). The NO_x range apparent from Figure 4 includes very low mixing ratios of a few pmol/mol, typically over the remote oceans, up to about 10 nmol/mol in polluted locations. At very low NO_x r asymptotes to about 0.15, reflecting OH recycling through the Cycle 2 mechanism (R9). At an r-value of about 0.6 there is a discontinuity toward the polluted regime where OH becomes insensitive to NO_x. At even higher NO_x r levels off at about 0.95. Note that in very polluted areas measured NO_x mixing ratios can sometimes exceed 10 nmol/mol. These concentrations do not occur in our model since emissions are released into relatively large grid boxes so that locally very high levels are artificially diluted. This means that in reality local r-values might even exceed 0.95, approaching 1, so that locally the system may become

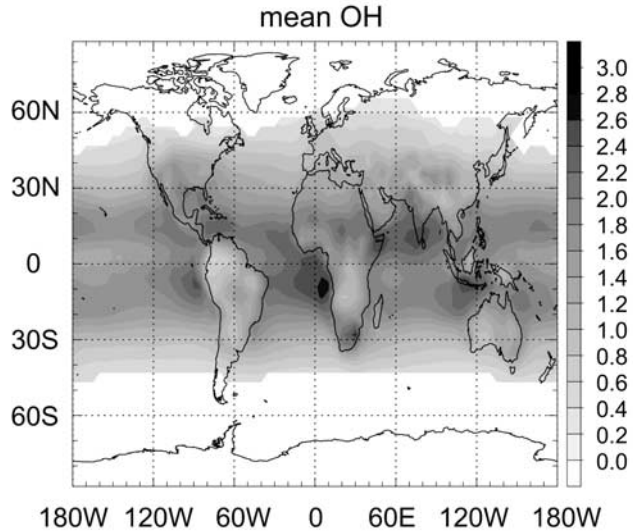

Figure 3. Model calculated annual mean OH in the present-day boundary layer in units of 10^6 molecules cm^{-3}, showing the domain in which primary OH production is most significant. In the white areas, i.e., outside the model domain discussed here, mean OH is less than 10^5 molecules cm^{-3}. Highest OH concentrations generally occur in regions where primary OH formation is strongest (controlled by O_3, UV and H_2O), and where OH sinks (e.g., by reactive carbon) are relatively small.

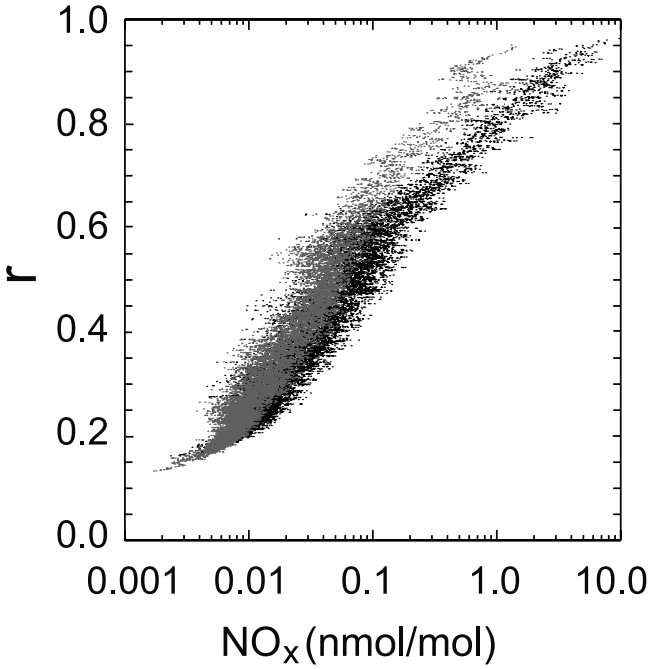

Figure 4. Model calculated annual average OH recycling probabilty (r) as a function of the ambient NO_x mixing ratio for all boundary layer grid boxes from one year of simulation. Black dots represent model results for present-day, grey for preindustrial conditions.

unstable, as mentioned above, although dilution is also a natural factor that limits such instabilities. Figure 5 presents the mean boundary layer OH recycling probability as a function of geographical location, showing that r is generally lowest in the marine troposphere ($r < 0.4$), while over the continents r is typically >0.5. Figure 5 also shows that the highest mean r-values occur over Europe and N-America, associated with strong NO_x emissions. Since primary OH formation is lower in Europe than in N-America (higher latitude; lower UV, T and H_2O) and the NO_x source density is highest in W-Europe, mean r in this region is highest in the world. From Figure 4 it is furthermore evident that r is a strong function of NO_x. For the free troposphere we obtain similar results although on average r is higher and the range is smaller, $0.35 < r < 0.85$, because the spread in NO_x is less.

[16] To investigate in which regions OH levels are most sensitive to perturbations we performed several sensitivity experiments. The objective was to approximate the total derivative dOH/dX for each grid box, thus extending the box model studies to the entire range of atmospheric conditions represented by our global model. For species X we selected CH_4 and NO_x since they have opposite effects, and because it is known that their sources have increased substantially. Figures 6a and 6b present results from two simulations, in which we perturbed the CH_4 and NO_x fields (separately). dCH_4 represents a 1% increase in the CH_4 mixing ratio at the surface. dNO_x has been simulated by adding a small NO source (of 0.014 molecules/cm^3/s) to each grid box. Additionally the NO emissions have been increased by 10^{-7} percent per time step because in polluted grid boxes the small fixed NO source is insignificant, hence

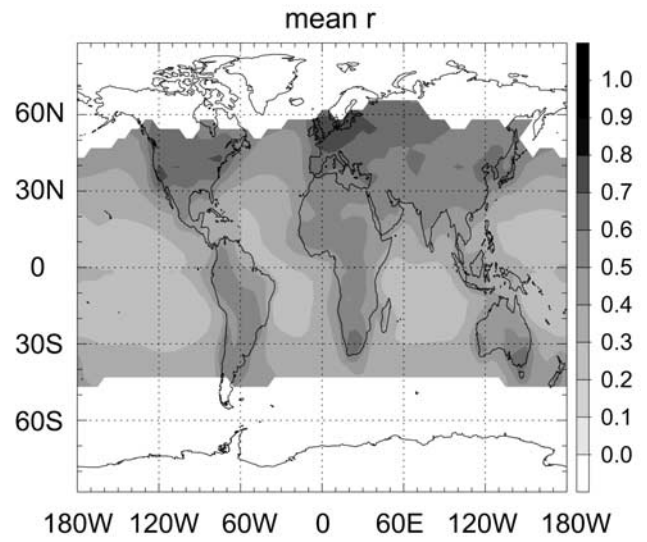

Figure 5. Model calculated annual mean OH recycling probability r in the boundary layer for the present-day simulation.

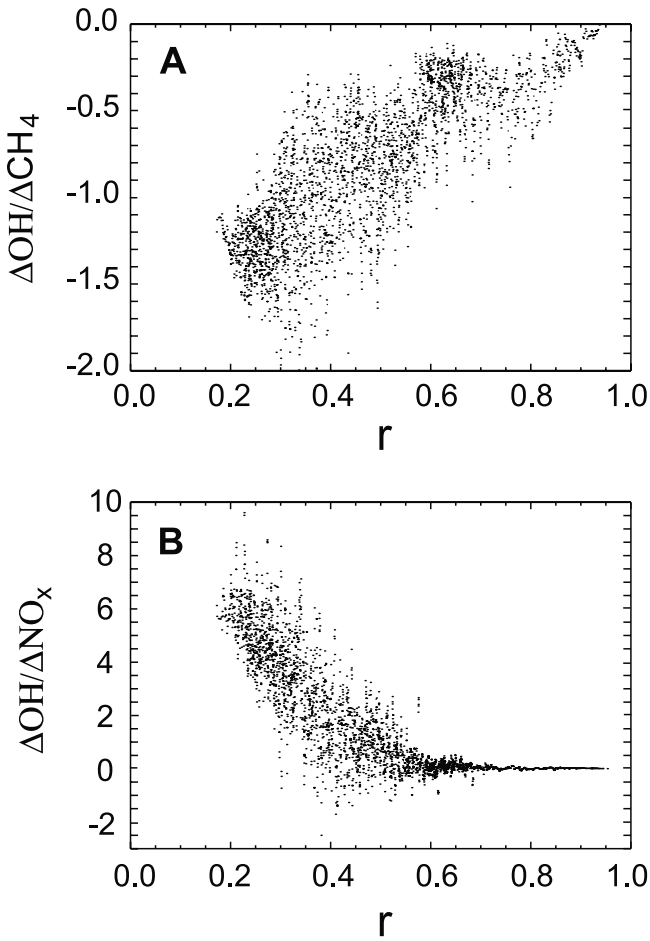

Figure 6. Model calculated OH changes caused by increases of (A) CH_4 (mol/mol $\times$ 10^8) and of (B) NO_x (mol/mol $\times$ 10^3) as a function of r. These results pertain to present-day conditions.

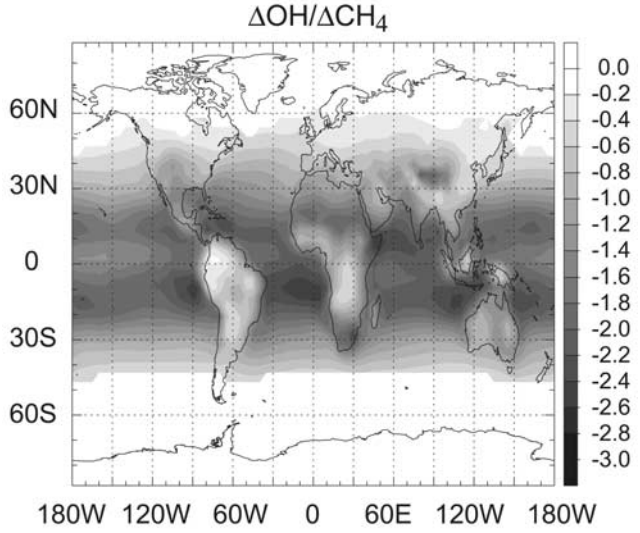

Figure 7. Model calculated OH changes caused by increases of CH_4 (mol/mol $\times$ 10^8) in the present-day boundary layer.

we simultaneously applied both constant and proportional perturbations. Transport effects of the short-lived NO_x perturbations were thus minimized, and the perturbations were chosen such that we expect only marginal effects on the overall chemistry. The difference terms $\Delta OH/\Delta CH_4$ and $\Delta OH/\Delta NO_x$, as presented in Figures 6, 7, and 8, have been calculated from the yearly average concentrations from the perturbed and unperturbed simulations.

[17] Hence increasing r renders the system less sensitive to small perturbations. The system appears to be relatively insensitive to perturbations at r-values above about 0.6. Although at $r \rightarrow 1$ the chemical system could become autocatalytical and unstable, such conditions do not occur in the model. At $r < 0.6$ the system is quite sensitive depending on ambient conditions. The system is most sensitive at about $r < 0.4$, mostly in low latitude marine locations, in particular in the southern tropics. Although the OH response to CH_4 and NO_x perturbations is not identical, the comparison of $\Delta OH/\Delta CH_4$ and $\Delta OH/\Delta NO_x$ in Figures 7 and 8 with the mean OH field in Figure 3 clearly shows that the system is generally most sensitive in regions in which OH concentrations are highest. In some continental regions with high NMHC concentrations, on the other hand, CH_4 perturbations have little effect. Figure 7 shows that over Amazonia, for example, isoprene levels are relatively high so that the small CH_4 perturbation applied only has a minor local influence on OH. Hence $\Delta OH/\Delta CH_4$ is small, also over other forested regions such as those in Africa and Indonesia (Figure 7).

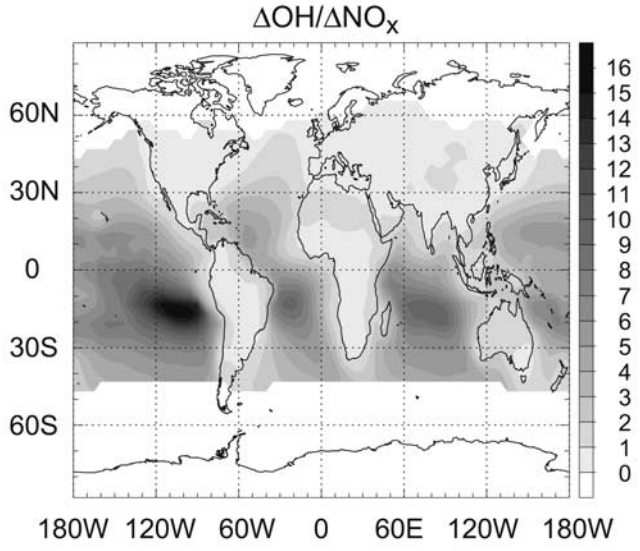

Figure 8. Model calculated OH changes caused by increases of NO_x (mol/mol $\times$ 10^3) in the present-day boundary layer.

[18] The sensitivity to NO_x perturbations is highest in the NO_x depleted regions over the tropical oceans where OH concentrations are nonetheless high. The most sensitive region is over the eastern Pacific Ocean at 10–20°S (Figure 8). In the subtropics the highest OH values are found in regions with strong NO_x emissions, high concentrations of O_3 and water vapor, or high photodissociation rates. One example is the Tibetan Plateau, where OH is also relatively sensitive to perturbations by CH_4 (Figure 7). The least sensitive regions are found over the polluted continents and high latitudes where OH recycling exceeds primary OH formation. An important implication of these results is that in NO_x depleted parts of the troposphere, i.e., far downwind of pollution sources, growing levels of reduced gases such as CH_4 and CO have the largest OH decreasing effect.

4. OH Distribution Changes

[19] Figure 2 shows the global mean HO_x cycles for both the preindustrial and present-day emission scenarios. Table 1 summarizes the global OH production rates, distinguishing the boundary layer from the free troposphere. We also differentiate between primary and secondary OH formation. By comparing these scenarios, it appears that global primary OH production has increased by about 50% from 62 to 92 Tmol yr^{-1}. Gross OH production increased even more strongly by more than 60% from 116 to 188 Tmol yr^{-1}. Hence increasing pollution has been accompanied by a 60% growth of the tropospheric oxidation power (defined as gross OH production). The global, diurnal mean OH abundance (volume weighted 1.1 $\times$ 10^6 molecules/cm^3), on the other hand, decreased merely about five percent. This

Table 1. Global Primary, Secondary, and Total Hydroxyl Formation

	Global P, Tmol yr^{-1}	Global S, Tmol yr^{-1}	Global total, Tmol yr^{-1}	Recycling probability (r)
		Preindustrial		
FT	37.1	40.7	77.8	0.52
BL	24.6	14.0	38.6	0.36
Total	61.7	54.7	116.4	0.47
		Present		
FT	54.2	67.0	121.2	0.55
BL	37.7	29.2	66.9	0.44
Total	91.9	96.2	188.1	0.51

FT is the free troposphere, BL is the boundary layer.

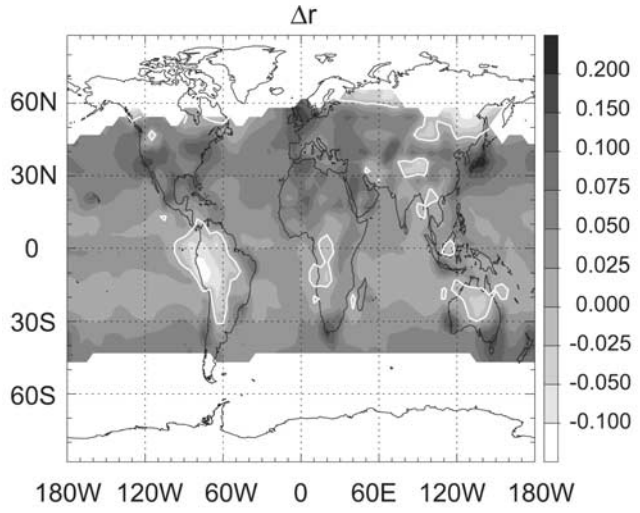

Figure 9. Model calculated annual mean change of the OH recycling probability *r* in the boundary layer, comparing the present-day with the preindustrial troposphere (*r* present minus *r* preindustrial). The white lines highlight the zero-contours.

relatively small OH change, considering that CH_4 and CO emissions have more than doubled, may suggest that global mean OH is not sensitive to perturbations. We argue, however, that global OH constancy should not be confused with OH stability.

[20] Previous modeling results have also indicated that mean OH has decreased less than 10% during the past century [*Lelieveld and Van Dorland*, 1995; *Wang and Jacob*, 1998]. Studies of the preindustrial holocene indicated that OH has remained within about 20% of its present value [*Pinto and Khalil*, 1991; *Crutzen and Brühl*, 1993; *Martinerie et al.*, 1995]. These modeling studies inferred that the relative constancy of mean OH during industrialization is associated with the correlation between the sources of NO_x and of CH_4 and CO. The concurrent growth of CH_4, CO and NO_x emissions has intensified OH recycling and O_3 formation in the troposphere, while increasing CH_4 and CO alone would have reduced global OH by at least a third [*Isaksen and Hov*, 1987; *Lelieveld and Van Dorland*, 1995; *Wang and Jacob*, 1998]. At present-day CH_4 and CO levels NO_x is quite efficient in recycling OH, in particular in the background troposphere (also because in low-*r* regions the NO_x lifetime has increased). Furthermore, the OH recycling probability *r* has increased over polluted regions, especially in the northern hemisphere, while changes of *r* over the remote oceans have merely been small. Figure 9 presents annual mean changes of *r* in the boundary layer, showing that these have been largest in the northern hemisphere in regions with strong NO_x emissions. Interestingly, Figure 9 suggests that the OH recycling probability decreased relatively strongly over the Amazon basin. Although primary OH production has increased owing to pollutant ozone formation, OH recycling is suppressed by the high isoprene concentrations so that *r* is substantially reduced.

[21] Although the global mean recycling probability has increased during the past century, on average from 0.47 to 0.51 (Table 1), Figure 4 shows that *r*-values as a function of NO_x have nevertheless decreased. The global increase of *r* results from the overall increased NO_x abundance. Globally, OH recycling has grown even more strongly than primary formation. Primary formation increased by nearly 50%, whereas OH recycling (i.e., secondary OH formation) increased by 75%, indicating a stability increase, at least globally averaged. The reduction of the recycling probability per NO_x molecule during industrialization is further illustrated by Figure 10, which shows the mean OH concentration as a function of NO_x, sampled from all boundary layer grid boxes. Figure 10 suggests that presently the OH optimum is reached at higher NO_x concentrations than in the preindustrial atmosphere. If an air mass contains more reactive carbon, more NO_x is required to attain the OH optimum and prevent radical-radical termination reactions. The decrease in OH sensitivity to NO_x in the 0.05–0.5 nmol/mol NO_x range, apparent from Figure 10, represents the reduced sensitivity of the system to perturbations, which is also seen in Figure 4 (notably for $r > 0.5$). Figure 10 furthermore shows that at low NO_x concentrations OH levels have decreased whereas under high NO_x conditions they have increased. The latter is a consequence of intensified primary OH formation associated with increasing O_3, while *r* has also increased because OH recycling has grown even more strongly.

[22] Figure 11 additionally presents OH changes between the present-day and preindustrial scenarios. Note that Figure 3 shows model calculated annual mean OH in the present-day boundary layer, and Figure 11 the fractional changes between preindustrial and present (ratio present/preindustrial OH). It illustrates the relatively large OH increases over the polluted continents, even though they are the most stable regions with the highest values of *r*. In these regions chemical perturbations are huge, associated with high photochemical O_3 production rates. In the background troposphere, in particular over the tropical oceans,

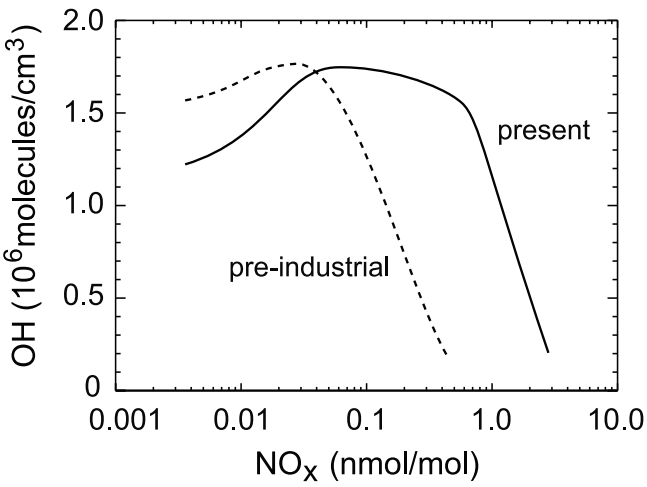

Figure 10. Average OH concentration as a function of ambient NO_x, calculated for the lower atmosphere. For NO_x depleted conditions (<40 pmol/mol; left of the curve crossing) the OH recycling efficiency has decreased during industrialization, whereas it has increased for NO_x enriched conditions.

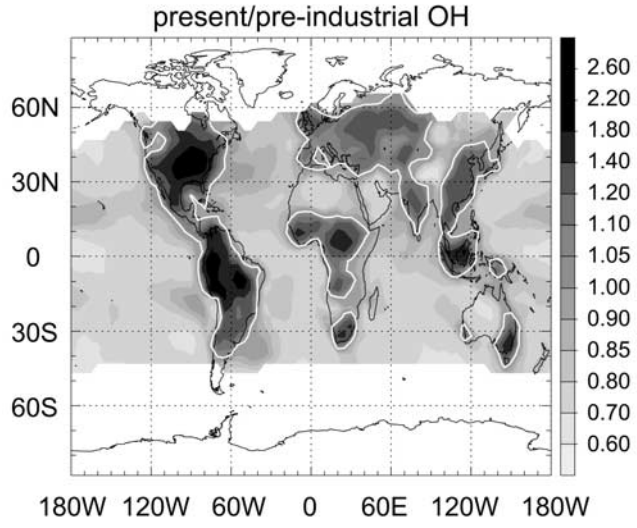

Figure 11. Model calculated fractional change of mean OH in the boundary layer, comparing the present-day with the preindustrial troposphere (OH present/preindustrial). OH has decreased over the oceans while it increased over the part of the continents where anthropogenic influences are strongest. The white lines highlight the 1.0-contours.

CH_4 and CO have increased substantially during the past century, whereas the concurrent increase of NO_x has been limited by its short lifetime. In these regions, therefore, the enhanced OH loss by reactions with CH_4 and CO predominates. On a global scale the positive and negative OH effects, over the continents and over the oceans, respectively, nearly cancel.

[23] From a long-term perspective global mean OH thus appears quite constant in time despite large-scale redistribution. The ''unintentional'' human practice to simultaneously emit nitrogen oxides and reactive carbon compounds from combustion processes has helped maintaining mean OH during industrialization. The global mean OH recycling probability has even slightly increased (Table 1). It should be emphasized, however, that global mean r cannot unequivocally characterize the system stability. The atmosphere is not an instantaneously mixed reservoir, in particular regarding slow inter-hemispheric exchange with a time constant of about a year. Moreover, in the background marine troposphere r has stayed approximately constant so that these regions have remained particularly sensitive to perturbations. In fact, increasing r in the polluted troposphere only moderately influences the system sensitivity, since r-values above about 0.6 are within a stable regime anyway (unless r would approach 1). Perturbations in the background troposphere, on the other hand, have a relatively larger influence, so that even small changes in reactive carbon concentrations have a relatively strong negative effect on OH.

5. Role of Transport

[24] In this section we use our scenario simulations to study to what extent the advection of OH precursors may have played a role in OH distribution changes. Though globally averaged $r \approx 0.5$, much lower r-values can occur in large areas, especially over the (sub)tropical oceans. The geographical distribution of r indicates that the system can be subdivided into the marine troposphere with values below about 0.45–0.5 and the continental troposphere with higher r-values (Figure 5). We therefore selected the global mean OH recycling probability of the preindustrial troposphere, $r = 0.47$, to serve as a threshold value between the high- and low-r regions (Table 2). This choice seems reasonable, bearing in mind that Δr is a measure of $\Delta \ln[NO_x]$, and that the principal NO_x increases in the past century have occurred over the continents. We have used the same area definition for the preindustrial and present troposphere so that the chemical budget calculations can be directly compared. The low-r area covers 67% and the high-r area 33% of the model domain considered, which encompasses 74% of the Earth's surface (where primary OH formation exceeds 0.55 nmol/mol s^{-1}). Note also that this partitioning is applied both to the boundary layer and the free troposphere although the transitions between the low and high-r regimes in the free troposphere are more diffuse owing to fast zonal transport. Table 2 presents the chemical budget terms for the low- and high-r regimes, for the boundary layer and the free troposphere, and for the present and preindustrial troposphere. The sum of these terms

Table 2. Primary (P) and Secondary (S) Hydroxyl Formation for Regions With Low r ($r \leq 0.47$) and High r ($r > 0.47$) Calculated for Preindustrial and Present-Day Emission Scenarios

	P, Tmol yr^{-1}		S, Tmol yr^{-1}									
	$O(^1D) + H_2O$		$NO + HO_2$		$O_3 + HO_2$		$H_2O_2 + h\nu$		$ROOH + h\nu$		Total S	
	BL	FT	BL	FT	BL	FT	BL	FT	BL	FT	BL	FT
						Low r						
preind	18.4	27.4	3.0	16.8	2.3	6.1	1.9	4.9	0.4	0.9	7.6	28.7
present	27.2	39.9	5.8	25.5	4.6	11.5	3.0	8.7	0.7	1.8	14.1	47.5
						High r						
preind	6.2	9.7	4.0	7.7	1.2	2.2	1.1	1.9	0.1	0.2	6.4	12.0
present	10.5	14.3	10.7	11.9	2.7	4.3	1.5	2.9	0.2	0.4	15.1	19.5
						Global						
preind	24.6	37.1	7.0	24.5	3.5	8.3	3.0	6.8	0.5	1.1	14.0	40.7
present	37.7	54.2	16.5	37.4	7.3	15.8	4.5	11.6	0.9	2.2	29.2	67.0

The low- and high-r analysis uses equal areas for both scenarios. FT is the free troposphere, BL is the boundary layer.

matches the total primary and secondary OH formation as listed in Table 1.

[25] As argued in section 4, the low *r*-values over the oceans indicate that CH_4 and CO increases in this part of the troposphere have a relatively large impact on OH. At low *r* the system is strongly dependent on primary OH formation. This is particularly the case in the marine boundary layer where primary OH formation typically exceeds secondary formation by a factor of two or more. For the NO_x depleted regions, where in situ photochemical O_3 loss dominates O_3 formation, transport of ozone appears to be very important [*De Laat and Lelieveld*, 2000]. Our model calculations show that under preindustrial conditions the low-*r* troposphere received a net amount of 12.7 Tmol yr^{-1} O_3 through advection. A fraction of 80% was from the stratosphere, highlighting the importance of stratosphere–troposphere exchange for the oxidation power of the background troposphere. The high-*r* troposphere imported as much ozone as it exported under preindustrial conditions. In the present-day troposphere, on the other hand, the high-*r* regions have become a net O_3 advection source, so that the low-*r* troposphere now receives 16.4 Tmol yr^{-1} O_3, an increase of about 30%. Note that under the low-*r* conditions the direct quantum yield from chemical O_3 loss is typically 1.8 OH (mostly through $O(^1D) + H_2O$ 2OH). Moreover, the additional OH enhances O_3 formation and thus primary OH production and recycling.

[26] The 30% increase of O_3 advection to the low-*r* troposphere in the past century helps to compensate the OH depletion caused by increasing CH_4 and CO, thus maintaining the oxidation power of the background troposphere. Ozone has a mean lifetime of several weeks so that rapid zonal transport leads to redistribution from polluted areas that are oxidant-enriched to remote areas that are oxidant-depleted. Ozone lives long enough to transfer the "NO_x effect" on a scale of thousands of kilometers while NO_x itself is rapidly removed in the vicinity of its sources. In section 4 we showed that OH has strongly increased in the high NO_x regions, thus limiting the NO_x lifetime and transport. Our model calculations nevertheless indicate that in the past century NO_x advection from high- to low-*r* regions increased from 42 to 127 Gmol yr^{-1}, being the result of a large NO_x emission increase by a factor of 3.5 (Gmol is 10^9 mol). Several other compounds also have an "oxidant transport potential", for example, peroxy acetyl nitrate (PAN) and other nitrates that act as reservoir species of NO_x [*Crutzen*, 1979; *Singh and Salas*, 1983; *Atlas*, 1988; *Atherton*, 1989]. PAN mostly releases NO_x in the relatively warm lower troposphere since it is thermally labile. Our model simulations suggest that PAN advection to the low-*r* regions increased from 111 to 231 Gmol yr^{-1}. Nitric acid is another NO_x reservoir species, which is more important for the upper troposphere (in the lower troposphere HNO_3 removal by deposition is very efficient). Advection of HNO_3 to low-*r* regions increased from 30 to 200 Gmol yr^{-1}.

[27] In the past century both primary and secondary OH production in the low-*r* troposphere have increased substantially (from 46 to 67 Tmol yr^{-1} and from 36 to 62 Tmol yr^{-1}, respectively). A significant fraction of the increased primary OH formation has been caused by enhanced ozone advection, about 7 Tmol yr^{-1}. Locally produced ozone increased by about 20 Tmol yr^{-1}, being compensated by increased chemical O_3 loss. The O_3 chemistry increase has also been caused by the growth of NO_x emissions within the region, from 171 to 398 Gmol yr^{-1}, in addition to the increase of NO_y advection by 375 Gmol yr^{-1} and of other O_3 precursors such as CH_4 and CO. As a consequence, the O_3 burden increased by 30% from 6 to 7.8 Tmol. The comparison of the present and preindustrial scenarios nevertheless shows that this O_3 increase, accompanied by enhanced primary and secondary OH formation, was not sufficient to prevent substantial OH depletion in the background troposphere.

6. Conclusions

[28] According to our modeling results and sensitivity studies, the global and long-term mean OH has remained close to about 10^6 molecules/cm^3 during the past century, however, the OH distribution has changed substantially. Over the polluted continents oxidant levels have increased strongly, associated with a decrease in air quality. Large-scale air pollution in the past century has been accompanied by a ~60% increase of the tropospheric oxidation power. Since global mean OH has remained approximately constant, this implies that the average OH lifetime has decreased by ~60%. In a previous study we have argued that, on a global scale, tropospheric ozone is controlled by in situ formation rather than by transport from the stratosphere, both in the present and preindustrial troposphere [*Lelieveld and Dentener*, 2000]. Globally, this exerts a stabilizing influence on OH, because an O_3 transport driven system would be strongly dependent on primary OH production, whereas in the chemistry dominated system OH recycling is equally important.

[29] Based on MCF analyses it has been suggested that OH changes during the past two decades may have been quite large. *Krol et al.* [1998] derived a positive global mean OH trend of nearly 0.5% yr^{-1} between 1978 and 1994. *Prinn et al.* [2001] inferred an even larger upward trend during the 1980s and a steep decline during the 1990s. Recent reanalysis of the MCF measurements, however, suggests that the large presumed OH changes, in particular the strong negative OH trend during the 1990s have been overestimated (Krol et al., submitted manuscript, 2002) [*Krol and Lelieveld*, 2002]. It is actually more likely that global mean OH has been rather constant. This does not necessarily mean, however, that the system is stable and that OH changes have been small. We must consider compensating effects of anthropogenic perturbations by reactive carbon and NO_x emissions, and redistribution of OH, which are hard to detect from MCF analyses. Hence global mean OH constancy is not the same as system stability. To determine the latter we also need to focus on smaller scales, associated with the limited lifetime of many substances that are not globally mixed. We have thus characterized the sensitivity of the OH chemical system through the OH recycling probability (*r*), a diagnostic calculated from primary and secondary OH formation. Although global mean *r* has slightly increased during the past century, we calculate large regional differences.

[30] Our modeling results indicate that the low latitude marine boundary layer is the most sensitive environment, characterized by a low OH recycling probability (low *r*).

Increases of CH_4 and CO have therefore strongly reduced OH here in the past century. In this part of the troposphere the system is increasingly dependent on oxidant advection to sustain OH formation. It appears that transport of O_3 and its precursors, notably reactive nitrogen species, plays an increasingly important role in the oxidation power of the background troposphere (i.e., the low-*r* troposphere). In the present troposphere long-range transport redistributes oxidant from photochemically polluted regions, being OH enriched, to OH depleted regions. This is not only important to supply oxidant for primary OH formation, it also contributes to OH recycling. Hence oxidant transport to the marine troposphere has thus prevented even larger OH depletion by increasing CH_4 and CO during the past century.

[31] In fact, oxidant transport away from the pollution sources is also important to maintain the stability of OH chemistry over the continents. Although these regions are characterized by a relatively high OH recycling probability, the huge perturbations by NO_x emissions have nevertheless caused strong OH increases. Without advective dilution, OH formation could locally become autocatalytic, leading to oxidant outbreaks, as predicted by box model studies and sometimes observed in very polluted conditions during summer [e.g., *Kleinman*, 1994]. It should be emphasized that even though the OH chemical system in the continental troposphere is more stable than over the oceans, regional perturbations, e.g., in Europe and the USA during the past century have been so large that OH could still change substantially. If the reactive carbon and NO_x emissions would not have taken place simultaneously, the OH changes might have been dramatic. Therefore, one should not conclude that in the most stable environments OH changes are small. Rather, if the system stability were low in these environments, OH changes would have been even much larger.

[32] Although our study has concentrated on the low and middle latitude troposphere where OH levels are highest, we note that the high latitude troposphere (>50° latitude), where primary OH formation is slow, is characterized by relatively high values of *r*, suggestive of a low sensitivity to perturbations (both preindustrial and present).

[33] We conclude that in regions where both the OH recycling probability is low and OH concentrations are high the system is sensitive to perturbations, i.e., in the low latitude marine troposphere. Moreover, the OH chemistry over the tropical rain forest in the Amazon has become more sensitive to perturbations. This underscores the importance of the tropics where future atmospheric changes will probably be largest, and where observations are particularly scarce (and thus urgently needed). Finally we emphasize that efforts by environmental protection agencies to limit NO_x emissions (to control smog, photochemical O_3, acid rain and eutrophication) contribute to a reduction of both OH and system stability unless CH_4 and CO emissions are reduced simultaneously. The latter should be pursued for many reasons, for example, to limit climate change.

References

Atherton, C., Organic nitrates in remote marine environments: Evidence for long-range transport, *Geophys. Res. Lett.*, *16*, 1289–1292, 1989.

Atlas, E., Evidence for $\geq C_3$ alkyl nitrates in rural and remote atmospheres, *Nature*, *331*, 426–428, 1988.

Chameides, W. L., and J. C. G. Walker, A photochemical theory of tropospheric ozone, *J. Geophys. Res.*, *78*, 8751–8760, 1973.

Crutzen, P. J., A discussion of the chemistry of some minor constituents in the stratosphere and troposphere, *Pure. Appl. Geophys.*, *106–108*, 1385–1399, 1973.

Crutzen, P. J., The role of NO and NO_2 in the chemistry of the stratosphere and troposphere, *Annu. Rev. Earth Planet. Sci.*, *7*, 443–472, 1979.

Crutzen, P. J., and C. Brühl, A model study of atmospheric temperatures and the concentrations of ozone, hydroxyl, and some other photochemically active gases during the glacial, the preindustrial holocene, and the present, *Geophys. Res. Lett.*, *20*, 1047–1050, 1993.

De Laat, A. T. J., and J. Lelieveld, Diurnal ozone cycle in the marine boundary layer, *J. Geophys. Res.*, *105*, 11,547–11,559, 2000.

Dentener, F. J., and P. J. Crutzen, Reaction of N_2O_5 on tropospheric aerosols: Impact on the global distributions of NO_x, O_3 and OH, *J. Geophys. Res.*, *98*, 7149–7163, 1993.

Dentener, F. J., J. Feichter, and A. Jeuken, Simulation of transport of Rn222 using on-line and off-line global models at different horizontal resolutions: A detailed comparison with measurements, *Tellus*, *51B*, 573–602, 1999.

Ehhalt, D. H., H.-P. Dorn, and D. Poppe, The chemistry of the hydroxyl radical in the troposphere, *Proc. R. Soc. Edinb., Ser. B.*, *97*, 17–34, 1991.

Ganzeveld, L., J. Lelieveld, and G. J. Roelofs, A dry deposition parameterization for sulfur oxides in a chemistry and general circulation model, *J. Geophys. Res.*, *103*, 5679–5694, 1998.

Gibson, R., P. Kallberg, and S. Uppsala, The ECMWF Re-Analysis (ERA) Project, *ECMWF Newsl.*, *73*, 7–11, 1997.

Guelle, W., Y. Balkanski, M. Schulz, F. Dulac, and P. Monfray, Wet deposition in a global size-dependent aerosol transport model, 1, Comparison of a 1 year 210Pb simulation with ground measurements, *J. Geophys. Res.*, *103*, 11,429–11,445, 1998.

Guthrie, P. D., The CH_4–CO–OH conundrum: A simple analytical approach, *Global Biogeochem. Cycles*, *3*, 287–298, 1989.

Hess, P., and S. Madronich, On tropospheric chemical oscillations, *J. Geophys. Res.*, *102*, 15,949–15,965, 1997.

Houweling, S., F. Dentener, and J. Lelieveld, The impact of nonmethane hydrocarbon compounds on tropospheric photochemistry, *J. Geophys. Res.*, *103*, 10,637–10,696, 1998.

Houweling, S., F. Dentener, and J. Lelieveld, Simulation of preindustrial atmospheric methane to constrain the global source strength of natural wetlands, *J. Geophys. Res.*, *105*, 17,243–17,255, 2000.

Isaksen, I. S. A., and O. Hov, Calculation of trends in the tropospheric concentration of O_3, OH, CO, CH_4 and NO_x, *Tellus*, *39B*, 271–285, 1987.

Kleinman, L. I., Low and high NO_x tropospheric photochemistry, *J. Geophys. Res.*, *99*, 16,831–16,838, 1994.

Krol, M. C., and J. Lelieveld, Can the variability in tropospheric OH be deduced from measurements of 1,1,1-trichlorethane (methyl chloroform)?, *J. Geophys. Res.*, *107*, doi:10.1029/2002JD002423, in press, 2002.

Krol, M. C., and D. Poppe, Nonlinear dynamics in atmospheric chemistry rate equations, *J. Atmos. Chem.*, *29*, 1–16, 1998.

Krol, M. C., P. J. van Leeuwen, and J. Lelieveld, Global OH trend inferred from methylchloroform measurement, *J. Geophys. Res.*, *103*, 10,697–10,711, 1998.

Landgraf, J., and P. J. Crutzen, An efficient method for online calculation of photolysis and heating rates, *J. Atmos. Sci.*, *55*, 863–878, 1998.

Lawrence, M. G., P. Jöckel, and R. von Kuhlmann, What does the global mean OH concentration tell us?, *Atmos. Chem.*, 37–49, 2001.

Lelieveld, J., and F. J. Dentener, What controls tropospheric ozone?, *J. Geophys. Res.*, *105*, 3531–3551, 2000.

Lelieveld, J., and R. van Dorland, Model simulations of ozone chemistry changes in the troposphere and consequent radiative forcings of climate during industrialization, in *Atmospheric Ozone as a Climate Gas*, *NATO ASI Ser.*, edited by W.-C. Wang and I. S. A. Isaksen, pp. 227–258, Springer-Verlag, New York, 1995.

Levy, H., II, Normal atmosphere: Large radical and formaldehyde concentrations predicted, *Science*, *173*, 141–143, 1971.

Logan, J. A., M. J. Prather, S. C. Wofsy, and M. B. McElroy, Tropospheric chemistry: A global perspective, *J. Geophys. Res.*, *86*, 7210–7354, 1981.

Martinerie, P., G. P. Brasseur, and C. Granier, The chemical composition of ancient atmospheres: A model study constrained by ice core data, *J. Geophys. Res.*, *100*, 14,291–14,304, 1995.

Marufu, L., F. Dentener, J. Lelieveld, M. Andreae, and G. Helas, Photochemistry of the African troposphere: The influence of biomass-burning emissions, *J. Geophys. Res.*, *105*, 14,513–14,530, 2000.

McConnell, J. C., M. B. McElroy, and S. C. Wofsy, Natural sources of atmospheric CO, *Nature*, *233*, 187–188, 1971.

Olivier, J. G. J., A. F. Bouwman, J. J. M. Berdowski, C. Veldt, J. P. J. Bloos, A. J. H. Visschedijk, C. W. M. van der Maas, and P. Y. J. Zandveld, Sectoral emission inventories of greenhouse gases for 1990 on a per country basis as well as on 1° × 1°, *Environ. Sci. Policy*, *2*, 241–264, 1999.

Perner, D., U. Platt, M. Trainer, G. Hübler, J. Drummond, W. Jünkermann, J. Rudolph, B. Schubert, A. Volz, and D. H. Ehhalt, Measurements of tropospheric OH concentrations: A comparison of field data with model predictions, *J. Atmos. Chem.*, *5*, 185–216, 1987.

Peters, W., M. Krol, F. Dentener, and J. Lelieveld, Identification of an El Niño-Southern Oscillation signal in a multiyear global simulation of tropospheric ozone, *J. Geophys. Res.*, *106*, 10,389–10,402, 2001.

Peters, W., M. Krol, F. J. Dentener, A. M. Thompson, and J. Lelieveld, Chemistry-transport modeling of the satellite observed distribution of tropical tropospheric ozone, *Atmos. Chem. Phys.*, *2*, 103–120, 2002.

Pinto, J. P., and M. A. K. Khalil, The stability of tropospheric OH during ice ages, interglacial epochs and modern times, *Tellus*, *43B*, 347–352, 1991.

Poppe, D., and H. Lustfeld, Nonlinearities in the gas phase chemistry of the troposphere: Oscillating concentrations in a simplified mechanism, *J. Geophys. Res.*, *101*, 14,373–14,380, 1996.

Prather, M., Lifetimes and eigenstates in atmospheric chemistry, *Geophys. Res. Lett.*, *21*, 801–804, 1994.

Prinn, R. G., et al., Evidence for substantial variations of atmospheric hydroxyl radicals in the past two decades, *Science*, *292*, 1882–1888, 2001.

Singh, H. B., and L. J. Salas, Peroxyacetylnitrate in the free troposphere, *Nature*, *302*, 326–328, 1983.

Spivakovsky, C. M., R. Yevich, J. A. Logan, S. C. Wofsy, M. B. McElroy, and M. J. Prather, Tropospheric OH in a three-dimensional chemical tracer model: An assessment based on observations of CH_3CCl_3, *J. Geophys. Res.*, *95*, 18,441–18,471, 1990.

Spivakovsky, C. M., et al., Three-dimendional climatological distribution of tropospheric OH: Update and evaluation, *J. Geophys. Res.*, *105*, 8931–8980, 2000.

Stewart, R. W., Dynamics of the low to high NO_x transition in a simplified tropospheric photochemical model, *J. Geophys. Res.*, *100*, 8929–8943, 1995.

Thompson, A. M., The oxidizing capacity of the Earth's atmosphere: Probable past and future changes, *Science*, *256*, 1157–1165, 1992.

Van Aardenne, J. A., F. J. Dentener, J. G. J. Olivier, and J. Lelieveld, A high resolution data set of historical anthropogenic trace gas emissions for the period 1890–1990, *Global Biogeochem. Cycles*, *15*, 909–928, 2001.

Wang, Y., and J. D. Jacob, Anthropogenic forcing on tropospheric ozone and OH since preindustrial times, *J. Geophys. Res.*, *103*, 31,123–31,135, 1998.

F. J. Dentener, Joint Research Centre, Environment Institute, TP280, I-21020 Ispra (Va), Italy.

M. C. Krol and W. Peters, Institute for Marine and Atmospheric Research, 3508 TA, Utrecht, The Netherlands.

J. Lelieveld, Max-Planck-Institute for Chemistry, P.O. Box 3060, D-55020 Mainz, Germany. (lelieveld@mpch-mainz.mpg.de)